

# Localized Crystallization of Calcium Phosphates by Light-Induced Processes

Patricia Besirske,<sup>[a]</sup> Arianna Menichetti,<sup>[b]</sup> Marco Montalti,<sup>\*,[b]</sup> Juan Manuel García-Ruiz,<sup>\*,[c]</sup> Martin Winterhalder,<sup>[a]</sup> Johannes Boneberg,<sup>[d]</sup> and Helmut Cölfen<sup>\*,[a]</sup>

Medical treatment options for bones and teeth can be significantly enhanced by taking control over the crystallization of biomaterials like hydroxyapatite in the healing process. Light-induced techniques are particularly interesting for this approach as they offer tremendous accuracy in spatial resolution. However, in the field of calcium phosphates, light-induced crystallization has not been investigated so far. Here, proof of principle is established to successfully induce carbonate-hydroxyapatite precipitation by light irradiation. Phosphoric acid is released by a photolabile molecule exclusively after irradiation, combining with calcium ions to form a calcium phosphate in the crystallization medium. 4-Nitrophenyl-

phosphate (4NPP) is established as the photolabile molecule and the system is optimized and fully characterized. A calcium phosphate is crystallized exclusively by irradiation in aqueous solution and identified as carbonate apatite. Control over the localization and stabilization of the carbonate apatite is achieved by a pulsed laser, triggering precipitation in calcium and 4NPP-containing gel matrices. The results of this communication open up a wide range of new opportunities, both in the field of chemistry for more sophisticated reaction control in localized crystallization processes and in the field of medicine for enhanced treatment of calcium phosphate containing biomaterials.

## Introduction

Living organisms, including humans, produce inorganic substances in the so-called biomineralization process, which has enabled an immense development in evolution.<sup>[1]</sup> Biominerals are produced to harden and stiffen tissues and are therefore used for various crucial roles, such as mechanical support and protection. Hydroxyapatite is the most prevalent biomineral in humans as it is the main component of human bones and teeth.<sup>[2]</sup> In today's medicine, huge efforts are made to

reconstruct bone defects. A vision for the future would be printing the personalized needed structure directly in the doctor's practice. Until now, prefabricated titanium implants are the method of choice due to their good corrosion resistance. Nevertheless, current studies prove that even titanium implants corrode in the body over time and the long-term influences of titanium ions are not fully understood yet.<sup>[3]</sup> An alternative implant material is polyether ether ketone (PEEK). The mechanical properties of PEEK are very similar to the ones of the bone, making it a potentially ideal implant material, however, it is entirely bio-inert and functionalization has to be performed for a successful osseointegration.<sup>[4]</sup> After implantation osseointegration of the implant must take place but the process is time-consuming and also not always successful; highlighting the need for further research in surface coatings.<sup>[4b]</sup> Besides metal implants, body-like materials can be used as implants. Calcium-deficient hydroxyapatite was reported as a compatible biomaterial.<sup>[5]</sup> However, large structures of foreign materials have to be implanted. A patient tailored implant of a smaller scale is desired. So far, personalized calcium phosphate implants are only accessible via a detour through cells, and a new technique to fabricate them with higher resolution is needed.<sup>[6]</sup> Here, we want to present a proof of principle to locally precipitate calcium phosphate by light irradiation. The use of light is especially suitable for this approach as the resolution of structures written by light is only depending on the wavelength  $\lambda$  of the light which is, without light scattering, on the nanometer to micrometer scale. This is a resolution being potentially by far higher than already known printing mechanisms.<sup>[7]</sup> Light-induced crystallization is already known in literature for calcium carbonate precipitation using ketoprofene as a photoinitiator for carbonate release.<sup>[8]</sup>

[a] P. Besirske, Dr. M. Winterhalder, Prof. Dr. H. Cölfen  
Physical Chemistry  
University of Konstanz  
Universitätsstr. 10, 78457 Konstanz (Germany)  
E-mail: helmut.coelfen@uni-konstanz.de

[b] Dr. A. Menichetti, Prof. Dr. M. Montalti  
Dipartimento di Chimica "Giacomo Ciamician"  
University of Bologna  
Via Selmi 2, 40126 Bologna (Italy)  
E-mail: marco.montalti2@unibo.it

[c] Prof. Dr. J. M. García-Ruiz  
Laboratorio de Estudios Cristalográficos Instituto  
Andaluz de Ciencias de la Tierra  
CSIC-Universidad de Granada  
Av. De las Palmeras 4, 18151 Armilla, Granada (Spain)  
E-mail: juanmanuel.garcia@csic.es

[d] apl. Prof. Dr. J. Boneberg  
Mesoscopic Systems, Department of Physics  
University of Konstanz  
Universitätsstr. 10, 78457 Konstanz (Germany)

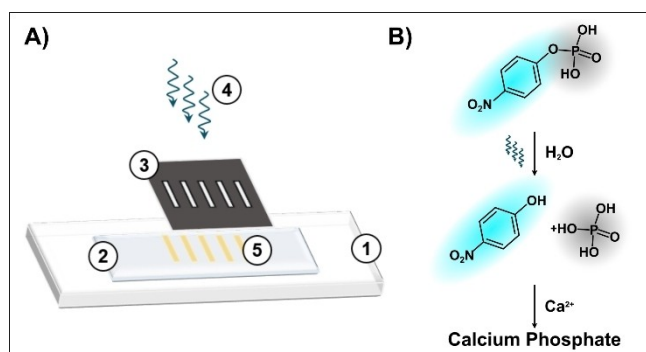
Supporting information for this article is available on the WWW under <https://doi.org/10.1002/chem.202302327>

© 2023 The Authors. Chemistry - A European Journal published by Wiley-VCH GmbH. This is an open access article under the terms of the Creative Commons Attribution License, which permits use, distribution and reproduction in any medium, provided the original work is properly cited.

## Results and Discussion

We have extended the approach from calcium carbonate to calcium phosphate using 4-Nitrophenylphosphate (4NPP) as the photolabile molecule releasing phosphate ions to precipitate calcium phosphate species in homogeneous solution as well as localized in a gel matrix (Scheme 1A).<sup>[9]</sup> The first proof of principle for precipitation was achieved in aqueous solution. 4NPP was dissolved besides  $\text{Ca}^{2+}$  from  $\text{CaCl}_2$ , and irradiated with UV light. This mechanism is shown in Scheme 1B leading to the release of free phosphoric acid/free phosphate ions. This effect is also visible in the significant drop in the pH value after irradiation (Figure 1, Supporting Information). Subsequently, the calcium ions precipitate in the presence of free phosphate as low-soluble calcium phosphate. The splitting process of 4NPP was analyzed via UV/Vis absorption spectroscopy. During kinetic experiments, a decrease of the absorption band at 312 nm occurs referring to the starting material 4NPP.<sup>[10]</sup> Additionally, an increase in the absorption band at 405 nm arises referring to the absorption band of the photo-byproduct 4-Nitrophenolate (4NP).<sup>[10a,c]</sup> This splitting was also confirmed by the  $^{13}\text{C}$ - and  $^{31}\text{P}$ -NMR spectra (Figure 2, Supporting Information). In accordance with the literature, the splitting reaction follows an exponential decay of a first-order reaction as seen in Figure 3A (Supporting Information).<sup>[11]</sup> With the data of the kinetic UV/Vis study, the photoreaction quantum yield of the splitting reaction was calculated to be 2% (Figure 4B, Supporting Information).

Having a closer look at both NMR spectra, after irradiation all signals of the non-irradiated spectrum are still present, suggesting that starting material has remained. Nonetheless, after irradiation in each NMR spectrum, one new signal has appeared. In the  $^{31}\text{P}$  spectrum, the signal at 0.20 ppm refers to the free phosphate ion, whereas the appearing signal at 168.28 ppm in the  $^{13}\text{C}$  spectrum refers to the emerging hydroxyl surrounding of the 4NP moiety after separation of the phosphate (Table 1, Supporting Information).<sup>[12]</sup> These findings, as well as the quantum yield analysis, were supported by the conducted titration studies (Figure 1A and B, Supporting Information). As there is a kink in the titration curve of the



**Scheme 1.** A) Schematic illustration of the irradiation and localization process of the gel: (1) glass slide; (2) gel matrix; (3) slit mask; (4) irradiation source; (5) irradiated regions. B) Irradiation of 4NPP with UV light leads to the byproduct 4NP (light blue) and phosphoric acid (grey) forming a calcium phosphate when calcium ions are present.

irradiated solution, whereas there is none in the titration curve of the non-irradiated solution, we propose that only after irradiation splitting occurs. The kink is not as distinct as in the reference with a free phosphate species represented by ammonium phosphate. Therefore, these studies are in accordance with the NMR, photoreaction quantum yield, and UV/Vis studies, all confirming a partial splitting of the starting material, exclusively after irradiation.

In the next step, we analyzed the precipitate of the irradiation process to ensure the formation of a calcium phosphate species. We proved via IR (Figure 1A) and pXRD (Figure 5, Supporting Information) measurements that the formed precipitate consists of amorphous calcium phosphate. As depicted in graph A of Figure 1 ten vibrational bands are distinguishable which are in conformity with values in the literature for carbonate apatite type B (Table 2, Supporting Information). pXRD measurements of the heated precipitate (Figure 1B) support the finding of the IR measurement as the measured diffractogram of the precipitate after heat treatment to 1000 °C is a superposition of carbonate-hydroxyapatite (COD 9003552), portlandite (COD 1001769), and calcium oxide (COD 9008605). The precipitate is only crystalline after a heating process, whereas it is amorphous directly after precipitation. An amorphous phase in the precipitation process is beneficial for

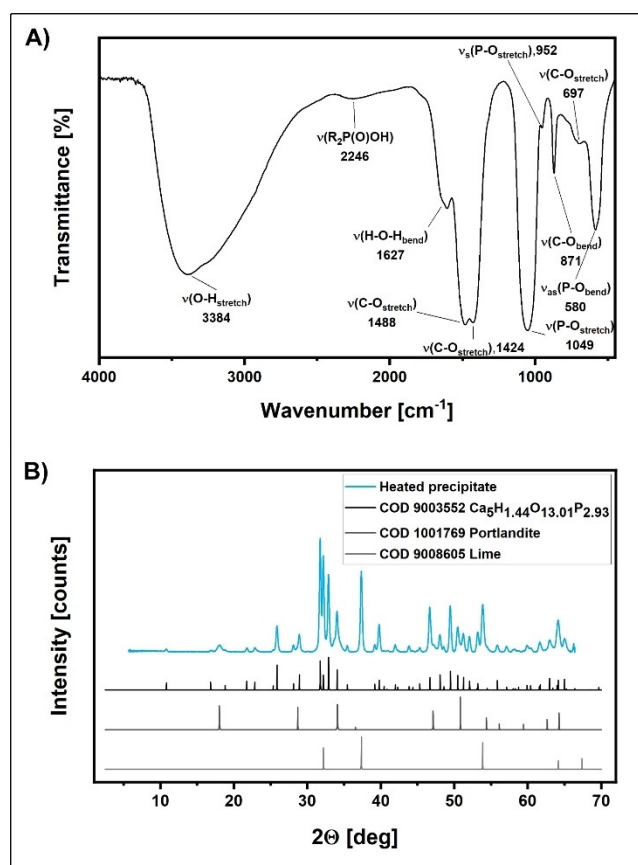


**Figure 1.** A) IR spectrum of the amorphous precipitate, including all significant bands of carbonate apatite type B.<sup>[14]</sup> B) pXRD spectrum of the heated precipitate and the references of carbonate-hydroxyapatite, portlandite, and calcium oxide (lime), the main components of the precipitate.

the subsequent application as an implant material, as the human body rearranges amorphous calcium phosphate towards crystalline self-reliantly.<sup>[13]</sup> SEM images of the temperature treated precipitate were taken which facilitate the finding of a homogenous particle size (Figure 6, Supporting Information). Moreover, we were able to tune the amount of carbonate present in the amorphous calcium phosphate by varying the amount of CO<sub>2</sub> available during the irradiation process and in the stock solutions (Figure 7, Supporting Information).

In the final step, we managed to confine the spatial resolution of the precipitation process using a gel matrix to slow down diffusion. Therefore, at first, the system had to be adapted to the new setup conditions. The calcium source as well as the 4NPP were included in the gel matrix via dialysis after the gelatinization process. Subsequently, the gel was irradiated with a frequency-tripled ns-pulsed Nd:YAG-laser (355 nm, energy density: 35 mJ/cm<sup>2</sup>). Irradiated areas turned yellowish, indicating the 4NPP was split into the byproduct 4NP, which absorbs at 405 nm, and a free phosphate. Masks were inserted into the beamline resulting in lithography-like patterns on the gel. After irradiation, the gels were washed and dried by lyophilization. In Figure 2A the SEM image of the gel is shown which exemplifies the characterization studies of the calcium phosphate inside the gel. Figure 2B and C show the EDX measurements of different elements, all recorded from the same area. It is visible that the calcium ion mapping (Figure 2C), as well as the phosphor ion mapping (Figure 2B), are following precisely the areas irradiated. Both show a higher elemental content in the irradiated areas in comparison to the non-irradiated areas. The irradiated areas can be recognized as the

wrinkled areas which appear due to the impact of the laser pulse.

In addition, Raman studies were performed as shown in Figure 2D to ensure the formation of a real mineral containing calcium and phosphor ions. Various calcium phosphate minerals feature a very predominant Raman vibration at 959 cm<sup>-1</sup>.<sup>[15]</sup> The precipitate of the aqueous light-induced precipitation process was analyzed to that effect and the vibration at 959 cm<sup>-1</sup> was present. Subsequently, the irradiated, in comparison to the non-irradiated areas of the gel, were analyzed via Raman, as the same calcium phosphate precipitate was assumed to be present. Reference measurements were conducted with the pure gel to exclude vibrations of the gel in the same region. Our measurements show that the gel matrices do not exhibit a vibration at this wavenumber. The spectrum of the non-irradiated area follows the spectrum of the pure gel, whereas the spectrum of the irradiated area shows a significant shoulder at 959 cm<sup>-1</sup>. These results, combined with the elemental mapping, confirm that not only a calcium phosphate has been formed but also that we were able to precisely confine the region of precipitation.

## Conclusions

In conclusion, we demonstrate a photolabile molecule, 4-Nitrophenylphosphate, releasing phosphate ions to locally precipitate calcium phosphate in a gel matrix. Incipiently, the aqueous system was fully characterized by UV/Vis, NMR, photo-reaction quantum yield, titration, and pH studies. We confirmed that the precipitation process is exclusively driven by UV light exposure. In the following, we were able to successfully identify the precipitate as amorphous carbonate apatite type B and subsequently after heating as crystalline carbonate-hydroxyapatite via XRD and IR measurements. Modification of the carbonate content was achieved by changing the CO<sub>2</sub> level during the precipitation process enabling a tunable final composition of the material. SEM, EDX, and TGA studies (Figure 8, Supporting Information) finalize the insights into the structure and decomposition mechanism of the precipitate. Afterwards, studies on the localization of the precipitate were conducted.

Our research led to the control over the localization and stabilization of the calcium phosphate achieved by a pulsed laser, triggering the precipitation inside a calcium containing gel matrix. The spatial resolution can currently be enhanced to 50 μm<sup>[8d]</sup> as reported for CaCO<sub>3</sub> but this was not in the focus of our current proof of principle study. The byproduct in the crystallization process is removable by washing or dialysis and therefore does not interfere with the organism, thinking of future applications. Additionally, it is noteworthy that the precipitate itself is amorphous which is beneficial for a subsequent application in the human body, as the human body remodels the carbonate apatite towards crystalline self-reliantly. At the current state of research, reaction times vary between hours to minutes depending on the irradiation system. As the present study is just proof of principle of the working

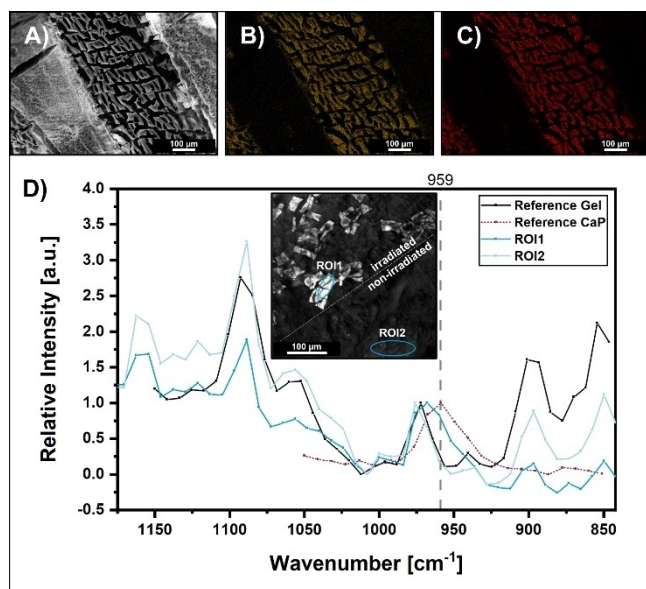


**Figure 2.** A) SEM image of the gel used for the EDX measurements after washing and drying procedure. B) Elemental mapping of the phosphor atoms. C) Elemental mapping of the calcium atoms. D) Raman measurements of irradiated and non-irradiated areas as well as a gel and calcium phosphate reference. The inset is showing the regions of interest used for the measurements.

mechanism, immediate use in medicine was not our goal. Nonetheless, we anticipate our results to be in principle transferable to other materials such as semiconductors and metals opening up a wide range of new opportunities; Either in the field of chemistry for more sophisticated reaction control in localized crystallization processes, generally applicable to medicine for an enhanced treatment of calcium phosphate containing biomaterials, as well as a sub-micron level of targeted metal deposition, for example, to be used in catalysis, as well as semiconductors for electronic applications.

## Supporting Information

The Supporting Information includes additional titration studies as well as pH measurements.  $^{13}\text{C}$  and  $^{31}\text{P}$  NMR spectra as well as UV/Vis kinetics are depicted. The UV/Vis spectra used for the calculation of the photochemical quantum yield are shown with the used calculation. The pXRD measurement of the untreated precipitate as well as additional SEM images, TGA, and IR spectra are shown. A table of each, the assigned IR vibrations, and NMR assignments, are attached. The Materials and Methods section as well as the used chemicals are shown.

Additional references cited within the Supporting Information.<sup>[16]</sup>

## Acknowledgements

The authors thank the European Research Council for funding project 101069348 – INPATT. Open Access funding enabled and organized by Projekt DEAL.

## Conflict of Interests

The authors declare no conflict of interest.

## Data Availability Statement

The data that support the findings of this study are available from the corresponding author upon reasonable request.

**Keywords:** biomineralization · calcium phosphate · materials science · photo-induced crystallization · photochemistry

- [2] a) S. V. Dorozhkin, *Prog. Biomater.* **2016**, *5*, 9–70; b) S. V. Dorozhkin, M. Epple, *Angew. Chem. Int. Ed.* **2002**, *41*, 3130–3146; c) H. El Feki, J. Michel Savariault, A. Ben Salah, M. Jemal, *Solid State Sci.* **2000**, *2*, 577–586; d) J. C. Elliott, in *Structure and Chemistry of the Apatites and Other Calcium Orthophosphates*, Elsevier Science, **1994**, p. 404.
- [3] a) J. J. Jacobs, A. K. Skipor, L. M. Patterson, N. J. Hallab, W. G. Paprosky, J. Black, J. O. Galante, *J. Bone Jt. Surg. Am. Vol.* **1998**, *80*, 1447–1458; b) R. Strietzel, A. Hösche, H. Kalbfleisch, D. Buch, *Biomaterials* **1998**, *19*, 1495–1499; c) A. Markowska-Szczupak, M. Endo-Kimura, O. Paszkiewicz, E. Kowalska, *Nanomaterials (Basel)* **2020**, *10*.
- [4] a) D. Almasi, N. Iqbal, M. Sadeghi, S. Izman, M. Abdulkadir, T. Zaman, *Int. J. Biomaterials* **2016**, *2016*, 1–12; b) J. Knaus, D. Schaffarczyk, H. Colfen, *Macromol. Biosci.* **2020**, *20*, e1900239.
- [5] T. Okuda, K. Ioku, I. Yonezawa, H. Minagi, Y. Gonda, G. Kawachi, M. Kamitakahara, Y. Shibata, H. Murayama, H. Kurosawa, T. Ikeda, *Biomaterials* **2008**, *29*, 2719–2728.
- [6] R. Raman, R. Bashir, in *Chapter 6 – Stereolithographic 3D Bioprinting for Biomedical Applications* (Eds.: A. Atala, J. J. Yoo), Academic Press, Boston, **2015**, pp. 89–121.
- [7] W. C. Liu, A. A. R. Watt, *Sci. Rep.* **2019**, *9*, 10766.
- [8] a) A. Menichetti, A. Mavridi-Prinzezi, G. Falini, P. Besirske, J. M. Garcia-Ruiz, H. Colfen, M. Montalti, *Chem. Eur. J.* **2021**, *27*, 12521–12525; b) T. Nishio, K. Naka, *J. Cryst. Growth* **2015**, *416*, 66–72; c) Y. Zhao, Y. Xie, S. Yan, Y. Dong, *Cryst. Growth Des.* **2009**, *9*, 3072–3078; d) M. H. Bistervels, M. Kamp, H. Schoenmaker, A. M. Brouwer, W. L. Noorduin, *Adv. Mater.* **2022**, *34*, e2107843.
- [9] P. Besirske, A. Menichetti, M. Montalti, J. Garcia-Ruiz, J. Boneberg, H. Colfen, *Goldschmidt 2022 (Hawaii)* **2022**, <https://doi.org/10.46427/gold2022.9630>.
- [10] a) A. Popov, A. Shcherbakov, N. Zholobak, A. Baranchikov, V. Ivanov, *Nanosyst.: Phys. Chem. Math.* **2017**, *8*, 760–781; b) J. Zhang, X. Lu, Y. Lei, X. Hou, P. Wu, *Nanoscale* **2017**, *9*; c) M. Mao, T. Tian, Y. He, Y. Ge, J. Zhou, G. Song, *Microchim. Acta* **2017**, *185*; d) J. Ma, X. Cheng, F. Peng, N. Zhang, R. Li, L. Sun, Z.-L. Li, H. Jiang, *J. Mater. Sci.* **2019**, *54*, 10055–10064.
- [11] a) K. Holbrook, L. Ouellet, *Can. J. Chem.* **1958**, *36*, 686–690; b) E. Havinga, R. Jongh, W. Dorst, *Recl. Trav. Chim. Pays-Bas* **2010**, *75*, 378–383.
- [12] a) [http://www.molbase.com/en/hnmr\\_100-02-7-moldata-32821.html](http://www.molbase.com/en/hnmr_100-02-7-moldata-32821.html), (accessed: 24.11.2020); b) R. W. McDowell, I. Stewart, *Chem. Ecol.* **2005**, *21*, 211–226.
- [13] A. Lotsari, A. K. Rajasekharan, M. Halvarsson, M. Andersson, *Nat. Commun.* **2018**, *9*, 4170.
- [14] F. Peters, in *Biologische Kristallisation von Calciumphosphaten – Untersuchung und Simulation, Doktorwürde*, Universität Hamburg, Hamburg, **2001**, p. 277.
- [15] a) G. R. Sauer, W. B. Zunic, J. R. Durig, R. E. Wuthier, *Calcif. Tissue Int.* **1994**, *54*, 414–420; b) <https://pocketdentistry.com/characterization-of-calcium-phosphates-using-vibrational-spectroscopies/>, (accessed: 16.10.2023).
- [16] a) L. Moggi, A. Juris, M. Gandolfi, in *Manuale del Fotochimico: Tecnique e metodologie. Bononia: Bononia*, University Press, **2006**, p. 208; b) T. Kaia, K. Gross, L. Plüduma, M. Veiderma, *J. Therm. Anal. Calorim.* **2011**, *110*, 647–659; c) M. Sneha, N. M. Sundaram, *Int. J. Nanomed.* **2015**, *10*, 99–106; d) [http://www.chemicalbook.com/SpectrumEN\\_4264-83-9\\_13C\\_NMR.htm](http://www.chemicalbook.com/SpectrumEN_4264-83-9_13C_NMR.htm), (accessed: 16.10.2023); e) L. Tortet, J. R. Gavarrí, G. Nihoul, A. J. Dianoux, *J. Solid State Chem.* **1997**, *132*, 6–16; f) M. Hesse, H. Meier, B. Zeeh, in *Spektroskopische Methoden in der organischen Chemie*, Georg Thieme Verlag, **2005**, p. 468; g) C. B. Baddiel, E. E. Berry, *Spectrochim. Acta* **1966**, *22*, 1407–1416; h) H. El Feki, C. Rey, M. Vignoles, *Calcif. Tissue Int.* **1991**, *49*, 269–274; i) M. Montalti, A. Credi, L. Prodi, M. T. Gandolfi, in *Handbook of Photochemistry*, CRC Press, **2006**, p. 664.

[1] a) T. Omokanwaye, O. C. Wilson, A. Gugssa, W. Anderson, *Mater. Sci. Eng. C* **2015**, *56*, 84–87; b) K. M. Towe, *Paleobiology* **1990**, *16*, 521–526.

Manuscript received: August 2, 2023

Accepted manuscript online: September 4, 2023

Version of record online: October 19, 2023